

Nanoscale

Accepted Manuscript



This is an *Accepted Manuscript*, which has been through the Royal Society of Chemistry peer review process and has been accepted for publication.

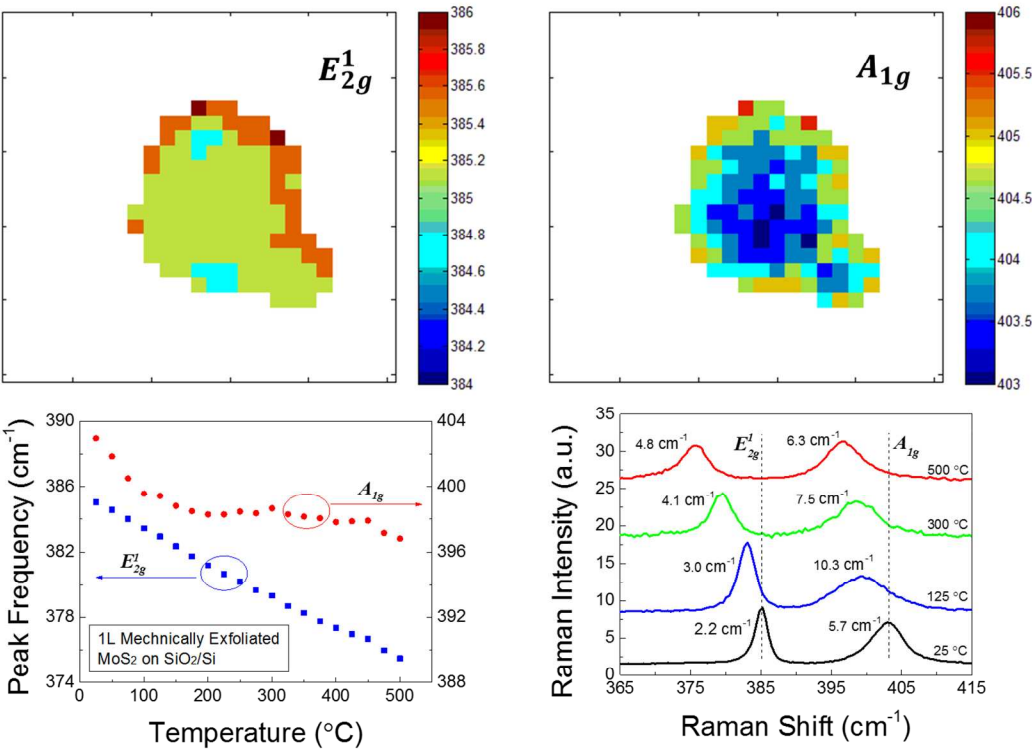
Accepted Manuscripts are published online shortly after acceptance, before technical editing, formatting and proof reading. Using this free service, authors can make their results available to the community, in citable form, before we publish the edited article. We will replace this *Accepted Manuscript* with the edited and formatted *Advance Article* as soon as it is available.

You can find more information about *Accepted Manuscripts* in the [Information for Authors](#).

Please note that technical editing may introduce minor changes to the text and/or graphics, which may alter content. The journal's standard [Terms & Conditions](#) and the [Ethical guidelines](#) still apply. In no event shall the Royal Society of Chemistry be held responsible for any errors or omissions in this *Accepted Manuscript* or any consequences arising from the use of any information it contains.

TOC

The coupling of quasi 2-D MoS₂ with substrate on different substrate type has been studied, probed by temperature dependent Raman scattering.



PAPER

Dependence of Coupling of Quasi 2-D MoS₂ with Substrate on Substrate Type, Probed by Temperature Dependent Raman Scattering

Cite this: DOI: 10.1039/x0xx00000x

Liqin Su,^a Yong Zhang,^{a,*} Yifei Yu,^b and Linyou Cao^bReceived 00th January 2012,
Accepted 00th January 2012

DOI: 10.1039/x0xx00000x

www.rsc.org/

This work reports a study on the temperature dependence of in-plane E_{2g}^I and out-of-plane A_{1g} Raman modes of single-layer (1L) and bi-layer (2L) MoS₂ films on sapphire (epitaxial) and SiO₂ (transferred) substrates as well as bulk MoS₂ single crystal in a temperature range of 25 – 500 °C. For the films on the transferred SiO₂ substrate, the in-plane E_{2g}^I mode is only weakly affected by the substrate, whereas the out-of-plane A_{1g} mode is strongly perturbed, showing highly nonlinear, sometimes even non-monotonic, temperature dependence in the Raman peak shift and linewidth. In contrast, for the films on the epitaxial sapphire substrate, E_{2g}^I is affected more significantly by the substrate than A_{1g} . This study suggests that the 2-D film-substrate coupling depends sensitively on the preparation method, and in particular on the film morphology for the transferred film. These findings are vitally important for the fundamental understanding and application of this quasi 2-D material that is expected to be supported by a substrate in most circumstances.

Introduction

Two-dimensional (2-D) materials such as graphene and hexagonal boron nitride (h-BN) have attracted tremendous attentions because of their extraordinary physical properties.^{1–6} However, graphene is a zero band gap material with vanishing density of states at the Dirac point, making it difficult to be used in electronic devices, particularly in transistors.⁷ Although several strategies of band gap engineering have been applied to open the band gap, generating a band gap larger than 400 meV remains a challenge.^{8–10} In contrast, h-BN has a band gap of 5.2 eV, too large for an efficient performance in electronic devices.¹¹ Recently, single-layer molybdenum disulfide (MoS₂), consisting of three atomic layers of one Mo and two S, has been shown to exhibit a direct band gap of ~1.8 eV, while bulk MoS₂ has an indirect band gap of 1.29 eV.^{12, 13} Since single-layer MoS₂ shares a number of common properties with graphene such as 2-D layered structure but has a finite band gap, it is considered to be an alternative to graphene, attracting a significant research interest. By using mechanical exfoliation method, single- and few-layer MoS₂ samples have been achieved, showing extremely strong photoluminescence compared to bulk MoS₂. Recently, single-layer MoS₂ based FETs have been reported to have a mobility of at least of 200 cm² V⁻¹ s⁻¹ and a current on/off ratio of 1×10^8 .¹⁴ These

promising optical and electronic properties can potentially lead to the development of high-quality low-power optoelectronic devices. Synthesis of large area of MoS₂ atomic layers has been demonstrated using a vapor-phase deposition method.¹⁵ Recently, it has been reported that a self-limiting approach can produce thin MoS₂ films over an area of centimeters with the layer number precisely controllable.¹⁶

A single-layer MoS₂ is formed by the arrangement of a triangular or simple hexagonal plane of Mo atoms sandwiched between two triangular layers of S atoms in a triangular prismatic fashion (see Fig.1(a)). Bulk MoS₂ is a periodically stacked S-Mo-S layers through Van der Waals force. The space group of single layer MoS₂ is $P6m2$ (point group D_{3h}), and the four first-order Raman active modes at the center of Brillouin zone are 32 cm⁻¹ (E_{2g}^2), 286 cm⁻¹ (A_{1g}), 383 cm⁻¹ (E_{2g}^I), and 408 cm⁻¹ (A_{1g}).^{17, 18} The E_{2g}^2 mode arises from the relative motion between two MoS₂ layers, which will vanish in the single layer sample. The E_{1g} mode is forbidden in back-scattering measurement on the basal plane perpendicular to the c axis. The E_{2g}^I mode is attributed to the in-plane relative motion between the two S atoms and the Mo atom, whereas the A_{1g} mode the out-of-plane vibration of two S atoms in opposite directions. Strictly speaking, the two active Raman modes E_{2g}^I and A_{1g} (in D_{6h} for bulk MoS₂) should be assigned as E' and A_1' in the monolayer MoS₂ (in D_{3h}).^{19, 20} However, to see the evolution

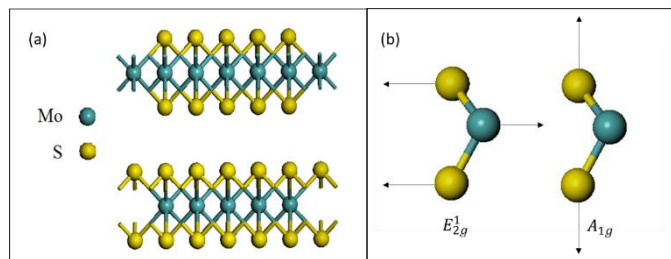


Fig. 1 (a) Schematic model of MoS₂ bulk and single layer. (b) In-plane phonon E_{2g}^1 and out-of-plane phonon A_{1g} for single-layer MoS₂.

from the bulk to single-layer,^{17, 21} the two modes are simply labelled as E_{2g}^1 and A_{1g} for all cases, as commonly done in the literature. Raman spectroscopy is a sensitive nondestructive technique to investigate structural and electronic properties of MoS₂. Similar to graphene, the Raman peak positions depend on the number of MoS₂ single layers, which makes it possible to determine the number of layers from Raman spectra.^{21, 22}

In this work, we report on the temperature dependent Raman spectra of both single- (1L) and bi-layer (2L) MoS₂, as well as the bulk sample. The knowledge of temperature dependent vibrational properties is important for further understanding electron-phonon interaction, transport properties, and crystal structure of material, which may largely impact the performance of electronic devices. Furthermore, because the MoS₂ is expected to be supported by a substrate in most if not all real applications, thus the coupling with substrate is inevitable, this temperature dependence study offers valuable insights to the effect of substrate, which might not be apparent at a fixed temperature. Since SiO₂/Si is widely used as the substrate for fabricating electronic devices after the film being

transferred from the original growth substrate, it is of particular interest to investigate the 2-D film with SiO₂/Si substrate.

The temperature variations of the Raman frequencies in MoS₂ on SiO₂/Si have been studied previously, giving the linear temperature coefficients, respectively, for E_{2g}^1 and A_{1g} modes: for few layers, -0.0132 cm⁻¹/K and -0.0123 cm⁻¹/K from 83 to 523 K;²³ for single layer, -0.0179 cm⁻¹/K and -0.0143 cm⁻¹/K from 300 to 550 K; and for bi-layer on, -0.0137 cm⁻¹/K and -0.0189 cm⁻¹/K from 300 to 550 K.²⁴ Apparently, the absolute and relative magnitudes of the temperature coefficients for the two modes differ significantly in these reported values. Furthermore, reliable data for the bulk MoS₂, which may serve as the references, are not readily available in the literature. The intrinsic mechanism for the redshift of Raman frequency with increasing temperature, as is known for most materials, is associated with the anharmonic effect due to weakening of the lattice potential energy.²⁵ In our work, we report the temperature dependent Raman measurements of single- and bi-layer MoS₂ in a larger temperature range from 300 to 773 K with small temperature increments, which allows us to accurately examine not only the nonlinearity of the temperature dependence but also the dependence of the film-substrate coupling on the substrate type.

Experimental Section

Samples

The samples investigated in this work have been obtained by two methods: mechanical exfoliation and chemical vapor deposition as reported in Ref.16. The 1L MoS₂ flake was mechanically exfoliated from nature crystalline bulk MoS₂ and

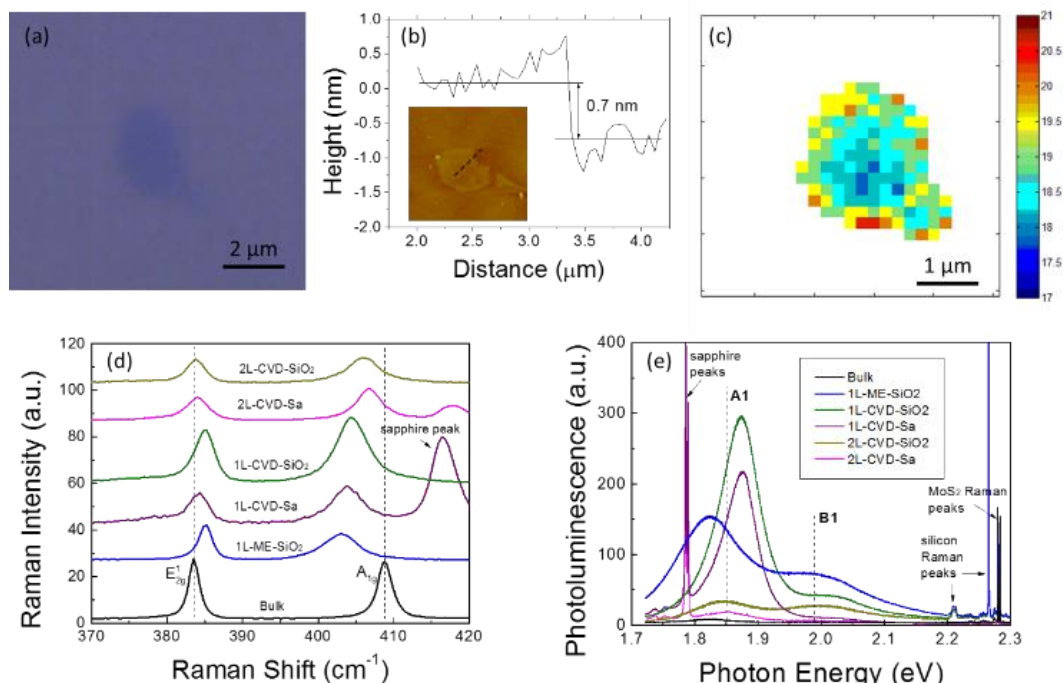


Fig. 2 Optical image (a) and AFM image (b) of mechanically exfoliated 1L MoS₂ on SiO₂/Si. (c) Map of the Raman frequency difference $\Delta\omega$, and the unit is cm⁻¹. (d) and (e) Raman and PL spectra of bulk MoS₂, and 1L and 2L on different substrates.

transferred onto a silicon wafer covered by a 300-nm-thick thermal oxide (SiO₂) layer (Sample 1L-ME-SiO₂). The CVD-grown 1L and 2L samples were prepared on two types of substrates, SiO₂/Si and sapphire labeled as, respectively, 1L-CVD-SiO₂, 1L-CVD-Sa, 2L-CVD-SiO₂, and 2L-CVD-Sa. Originally the MoS₂ films were grown on sapphire wafers, and then transferred to SiO₂/Si wafers by scotch tape. Raman system used in this work is Horiba LabRam HR800 with a spectral resolution smaller than 1 cm⁻¹. A 532 nm laser was used with power ~1 mW, low enough to avoid heating of the samples. The temperature dependent measurements were performed with a 50× long-working-distance lens.

Characterization of Samples

Fig.2(a) shows the optical image of an exfoliated 1L MoS₂ film on the SiO₂/Si wafer, with an AFM image in Fig.2(b), confirming the one-layer thickness which is ~0.7 nm. The Raman frequency difference ($\Delta\omega$) between the E_{2g}^1 and A_{1g} modes has been shown to correlate with the layer number, with $\Delta\omega = 19$ cm⁻¹ for 1L and 22 cm⁻¹ for 2L.²¹ Raman mappings of exfoliated films were carried out to examine the thickness distribution of the MoS₂ film at room temperature, and the spatial variation of the frequency difference $\Delta\omega$ is shown in Fig.2(c). All the $\Delta\omega$ values are found less than 20 cm⁻¹, indicating it is indeed single-layer MoS₂. Room temperature Raman and photoluminescence (PL) spectra of all the samples, including a bulk MoS₂ sample, used in this work are shown in Fig.2(d) and 2(e), respectively. With increasing number of layers, the E_{2g}^1 peak shows a redshift in Raman frequency while A_{1g} peak blueshift. There are small shifts in the peak position among samples of the same thickness but on different substrates, due to residue strain, suggesting some coupling between the film and substrate. In addition, the linewidths of 1L and 2L samples are somewhat larger than those of the bulk sample, which could be an indication of inhomogeneity of the strain. It has been reported that the PL of MoS₂ has two peaks that correspond to A1 (1.85 eV) and B1 (1.98 eV) direct excitonic transitions of MoS₂.¹³ The A1 and B1 transitions are, respectively, at 1.82 eV and 1.98 eV for sample 1L-ME-SiO₂, 1.87 eV and 2.0 eV for single-layer CVD samples, and 1.85 eV and 1.99 eV for bi-layer CVD samples. The variation of PL peak positions of MoS₂ samples could be due to the interaction between the film and the substrate and possibly impurities in the films. Additionally, the 1L MoS₂ samples show the strongest PL signal, while bulk MoS₂ negligible, as expected due to the electronic band structure change.

Experimental Setup

For the temperature dependent study, a Linkam TS1500 heating system, with a temperature control accuracy of 1 °C, was used to heat the samples with a step of 25 °C, and heating rate of 10 °C/min. Five minutes was applied to hold the temperature at each temperature step, allowing sufficient time for stabilization. An extremely low flow rate of nitrogen gas was purged to avoid the oxidization of MoS₂ into MoO₃. After the sample temperature stabilized, Raman spectra were acquired by the

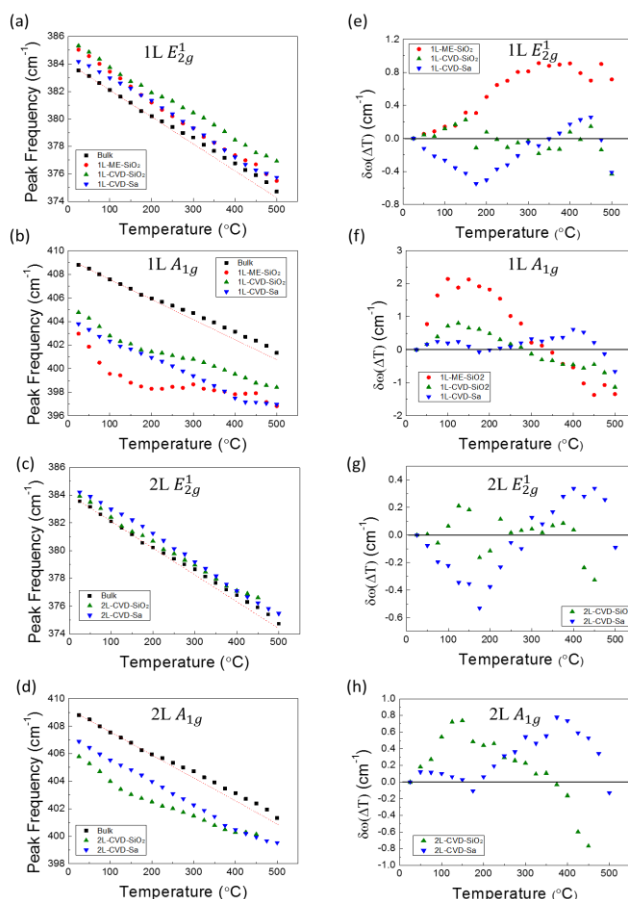


Fig. 3 (a)-(d) Temperature dependence of Raman frequencies of E_{2g}^1 and A_{1g} modes in bulk and all other 1L and 2L samples. (e)-(h) The Raman frequency deviation of 1L and 2L MoS₂ relative to bulk MoS₂ as the reference.

Horiba Raman system. A few samples were heated in the ambient environment, and no Raman signals of E_{2g}^1 and A_{1g} modes were observed when the temperature > 350 °C, implying total oxidization of MoS₂ films.

Results and discussion

Temperature dependence of Raman scattering

The temperature dependences of both E_{2g}^1 and A_{1g} peak positions were performed in the range from room temperature (25 °C) to 500 °C, shown in Fig.3(a)-(d). The upper temperature range in this work is substantially higher than those in the previous works < 250 °C.^{23, 24} The results of bulk MoS₂ are used as a reference. Empirically, the temperature dependence of Raman shift can be described by:

$$\omega(\Delta T) = \omega_0 + \chi_1 \Delta T + \chi_2 (\Delta T)^2 + \chi_3 (\Delta T)^3, \quad (1)$$

where ω_0 is the frequency at room temperature, ΔT is the temperature change relative to room temperature, and χ_1 is the first-order temperature coefficient. The second (χ_2), third (χ_3) or higher order temperature effects are usually assumed to be small in the literature. In reality, the nonlinear effects are found to be quite significant for 1L or 2L MoS₂ even in a temperature

range where the linear dependence might be expected to be adequate, for instance, below 200 °C, depending on the substrate. Even for bulk MoS₂, the nonlinearity occurs at around 200 °C for both E_{2g}^l and A_{1g} , though rather weak, but nevertheless evident in our data. It is perhaps reasonable to assume that the temperature shift for a free standing few-layer MoS₂ should be rather close to that of the bulk material, despite the difference in the absolute position. Therefore, to show more clearly the substrate effect, we can take the temperature shifts of the bulk sample as references. Fig.3(e)-(h) plot the difference in the Raman frequency shifts between the thin film sample and the bulk, $\delta\omega(\Delta T) = |\omega(\Delta T) - \omega_0|_{\text{thin film}} - |\omega(\Delta T) - \omega_0|_{\text{bulk}}$, for E_{2g}^l and A_{1g} and for 1L and 2L samples. Below we discuss separately E_{2g}^l and A_{1g} to examine the effects of two types of substrates.

(1) E_{2g}^l : For both the 1L and 2L samples, as shown in Fig.3(a) and (c), Fig.3(e) and (g), the E_{2g}^l mode exhibits relatively weak nonlinearity or in general appears to be close to the temperature dependences of the bulk sample. The temperature dependences of the deviations from the bulk mode are qualitatively similar for the same type of substrate: 1L-CVD-Sa and 2L-CVD-Sa vs. 1L-CVD-SiO₂ and 2L-CVD-SiO₂, which is more apparent in Fig.3(e) and (g), due to subtle difference in the film-substrate coupling (to be discussed later). The deviations of 1L-ME-SiO₂ are somewhat different from the other samples, as shown in Fig.3(e).

(2) A_{1g} : For both 1L-ME-SiO₂ and 1L-CVD-SiO₂, as shown in Figs.3(b) and (f), the temperature dependence of A_{1g} mode is drastically different from that of the bulk, showing strong nonlinearity starting at temperature near 100 °C and an overall 'S' shape dependence. The Raman spectra of 1L-ME-SiO₂ at a few representative temperatures are shown in Fig.4. The FWHM of A_{1g} mode is 5.7 cm⁻¹ at room temperature, increasing to a maximum of 10.3 cm⁻¹ at around 125 °C, then it decreases to 6.3 cm⁻¹ when the temperature reaches 500 °C, whereas the FWHM of E_{2g}^l mode increases from 2.2 cm⁻¹ at room temperature monotonically to 4.8 cm⁻¹ at 500 °C. However, 1L-

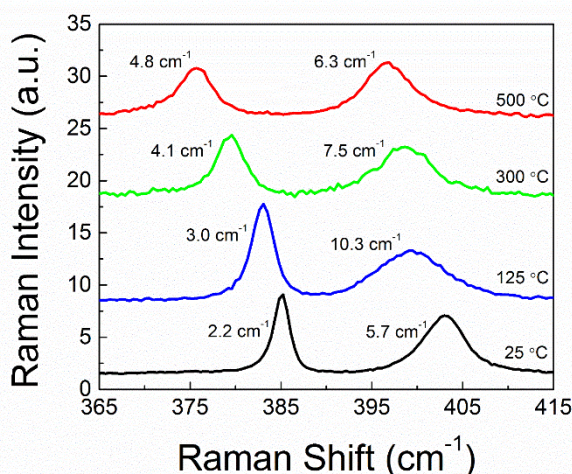


Fig. 4 Representative Raman spectra of 1L-ME-SiO₂ sample at particular temperatures. The FWHM of E_{2g}^l and A_{1g} are labelled besides the peaks.

CVD-Sa shows only small deviation from the bulk dependence, with an average slope of -0.0159 cm⁻¹/K by using linear fitting, up to 425 °C, then an obvious change occurs, becoming nearly flat with a slope of -0.0027 cm⁻¹/K. As for the 2L samples, Fig.3(d) and (h), similar to 1L-CVD-SiO₂, 2L-CVD-SiO₂ exhibits more significant deviation from the bulk sample than 2L-CVD-Sa when temperature < 400 °C. For 2L-CVD-Sa, the slope changes significantly when T > 400 °C from -0.0162 cm⁻¹/K to -0.0102 cm⁻¹/K. Again, one may notice that the temperature dependences of the deviations from the bulk mode are qualitatively similar for the same type of substrate: 1L-CVD-Sa and 2L-CVD-Sa vs. 1L-CVD-SiO₂ and 2L-CVD-SiO₂, which is more apparent in Fig.3(f) and (h).

Visually from Fig.3(a)-(d), the A_{1g} mode shows more nonlinearity than the E_{2g}^l mode. Qualitatively similar results have been observed in graphene: the peak position of G band, an in-plane vibrational mode, is less susceptible to the substrate influence than an out-of-plane vibration mode ~861 cm⁻¹.^{26, 27} Similarly it is reasonable to expect that in MoS₂ the in-plane mode (E_{2g}^l) will be less affected by the interaction between film and substrate than the out-of-plane mode (A_{1g}). Thus, it is not difficult to understand that the E_{2g}^l mode typically shows more linear temperature dependent Raman shift than A_{1g} mode for both 1L and 2L samples. The difference between the SiO₂ and sapphire substrate also indicates that the coupling between the film and substrate depends on the substrate type and/or how the film and substrate is bound.

The temperature coefficients of all the samples are fitted to third order with polynomial function according to Eq.(1), listed in Table 1. The linear temperature coefficients of E_{2g}^l and A_{1g} in bulk MoS₂ are $\chi_1 = -0.0221 \pm 8.9 \times 10^{-4}$ cm⁻¹/K and $-0.0197 \pm 8.9 \times 10^{-4}$ cm⁻¹/K, respectively. Bulk MoS₂, as the reference, can be treated as a stacking of single-layered MoS₂ films, and each layer has the same properties. With increasing temperature, all layers expand with the same rate without introducing any strain, leading to a nearly linear redshift of the Raman peak position for both E_{2g}^l and A_{1g} modes. Although the interlayer coupling has led to significant frequency shifts for the two modes between 1L and bulk, the changes in temperature coefficients are expected to be relatively small. For the E_{2g}^l mode, the first-order temperature coefficients (χ_1) of SiO₂ samples, both 1L and 2L, are close to that of bulk MoS₂, while those of the sapphire samples are much smaller. For A_{1g} , all the SiO₂ samples yield much larger χ_1 's than that of bulk MoS₂, while sapphire samples are close to bulk MoS₂. Our results for the films on SiO₂/Si are contradicting to or significantly different from those reported in the literature, because the improved data accuracy allows to examine the nonlinear effect that was neglected.^{23, 24}

Because all the SiO₂ samples were produced by mechanical exfoliation, it is possible that wrinkles or ripples were introduced to the films, resulting in a considerable strain in the film.²⁸ Fig.5 gives the spatial maps of the Raman frequencies of E_{2g}^l and A_{1g} modes for mechanically exfoliated single-layer MoS₂ film on SiO₂/Si (1L-ME-SiO₂) at room temperature. The maps demonstrate that the frequency of A_{1g} show a larger

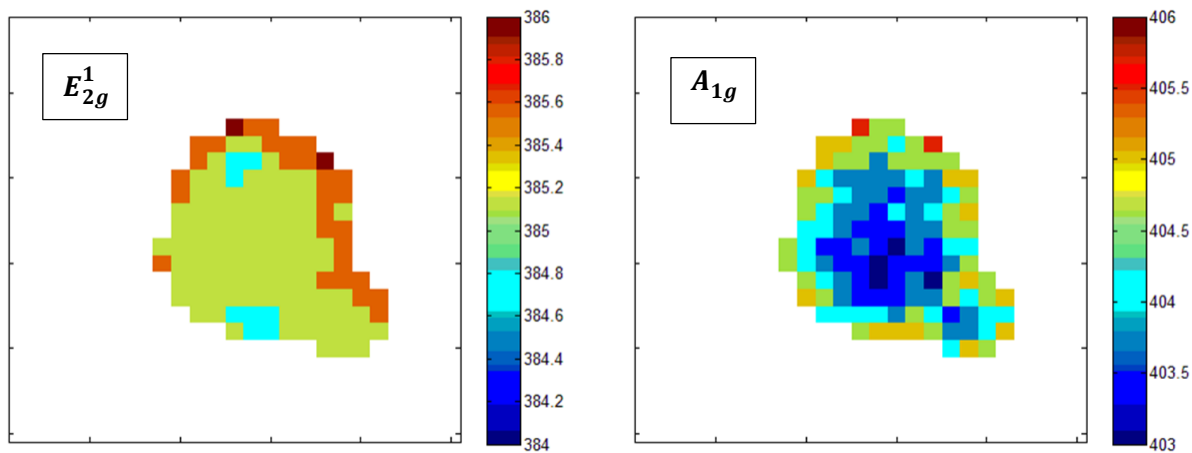


Fig. 5 Spatial maps (6 $\mu\text{m} \times 6 \mu\text{m}$) of the Raman frequencies of (a) E_{2g}^1 and (b) A_{1g} modes for 1L-ME-SiO₂ sample, and the unit is cm^{-1} .

Table 1 Temperature coefficients of bulk, 1L and 2L samples with polynomial fitting to third order.

		χ_1	χ_2	χ_3
E_{2g}^1	bulk	$-0.0221 \pm 8.9 \times 10^{-4}$	$2.12 \times 10^{-5} \pm 4.4 \times 10^{-6}$	$-2.94 \times 10^{-8} \pm 6.1 \times 10^{-9}$
	1L-ME-SiO ₂	-0.0241 ± 0.0015	--	--
	1L-CVD-SiO ₂	-0.0217 ± 0.0017	$2.04 \times 10^{-5} \pm 8.4 \times 10^{-6}$	$-2.68 \times 10^{-8} \pm 1.2 \times 10^{-8}$
	1L-CVD-Sa (till 425 °C)	$-0.0143 \pm 5.7 \times 10^{-4}$	$-1.44 \times 10^{-5} \pm 3.4 \times 10^{-6}$	$7.71 \times 10^{-9} \pm 5.6 \times 10^{-9}$
	2L-CVD-SiO ₂ (till 400 °C)	-0.0233 ± 0.0018	$3.00 \times 10^{-5} \pm 1.1 \times 10^{-5}$	$-4.61 \times 10^{-8} \pm 2.0 \times 10^{-8}$
	2L-CVD-Sa (till 425 °C)	$-0.0135 \pm 8.4 \times 10^{-4}$	$-2.54 \times 10^{-5} \pm 5.0 \times 10^{-6}$	$2.93 \times 10^{-8} \pm 8.2 \times 10^{-9}$
	1L ME SiO ₂ Ref. ²⁴	-0.0179		
	2L ME SiO ₂ Ref. ²⁴	-0.0137		
	few layer Ref. ²³	-0.0132		
A_{1g}	bulk	$-0.0197 \pm 8.9 \times 10^{-4}$	$2.49 \times 10^{-5} \pm 4.4 \times 10^{-6}$	$-3.53 \times 10^{-8} \pm 6.1 \times 10^{-9}$
	1L-ME-SiO ₂	-0.0626 ± 0.0038	$2.11 \times 10^{-4} \pm 1.7 \times 10^{-5}$	$-2.34 \times 10^{-7} \pm 2.1 \times 10^{-8}$
	1L-CVD-SiO ₂	-0.0301 ± 0.0023	$8.15 \times 10^{-5} \pm 1.1 \times 10^{-5}$	$-1.00 \times 10^{-7} \pm 1.6 \times 10^{-8}$
	1L-CVD-Sa (till 425 °C)	-0.0199 ± 0.0012	$3.10 \times 10^{-5} \pm 7.2 \times 10^{-6}$	$-5.77 \times 10^{-8} \pm 1.2 \times 10^{-8}$
	2L-CVD-SiO ₂ (till 400 °C)	-0.0310 ± 0.0018	$8.56 \times 10^{-5} \pm 1.2 \times 10^{-5}$	$-1.16 \times 10^{-7} \pm 2.0 \times 10^{-8}$
	2L-CVD-Sa (till 425 °C)	-0.0160 ± 0.0014	--	--
	1L ME SiO ₂ Ref. ²⁴	-0.0143		
	2L ME SiO ₂ Ref. ²⁴	-0.0189		
	few layer Ref. ²³	-0.0123		

variation than that of E_{2g}^1 , indicating that the morphology of the film impacts the Raman frequency of A_{1g} more than that of E_{2g}^1 . On the other hand, both 1L and 2L MoS₂ films were originally grown on sapphire. It has been reported, for graphene, the possibility of forming bonds between mechanically exfoliated graphene and substrate is quite low; however, such bonds are

possible with high-temperature growth.²⁹ It is reasonable to believe that the CVD growth of MoS₂ films at the temperature higher than 800 °C could produce somewhat stronger bonding between the MoS₂ film and sapphire substrate than in the case of transferred film. With increasing temperature, the chemical bonding would influence the in-plane vibration, giving rise to a

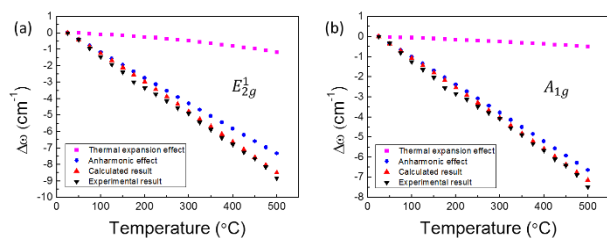


Fig. 6 The model of temperature dependent Raman shift relative to room temperature including the contributions of thermal expansion effect of lattice and anharmonic effect as compared to experimental results of bulk MoS₂ for (a) E_{2g}^1 and (b) A_{1g} modes.

damping of Raman frequency redshift to E_{2g}^1 mode at the low temperature region, as manifested on the reduced magnitude of χ_1 for the CVD-grown MoS₂ films on sapphire. Furthermore, the film-substrate coupling leads to the sign changes for both χ_2 and χ_3 compared to the bulk for the E_{2g}^1 mode of the on-sapphire samples. In contrast, mechanically transferred MoS₂ films on SiO₂/Si do not form the chemical bonding between film and substrate other than Van der Waals force, leading to the temperature dependence of Raman shift or χ_1 of the E_{2g}^1 mode similar to bulk MoS₂. However, the MoS₂ films on SiO₂/Si are more likely to be affected by the changes in the film morphology such as wrinkles and ripples when temperature increases, due to thermal expansion coefficient mismatch between MoS₂ and SiO₂. These changes of morphology in turn will have a large impact on out-of-plane vibration (A_{1g}), causing not only the nonlinear effect of temperature coefficient but also the large deviation of χ_1 from bulk MoS₂ for the SiO₂/Si samples. As for the sapphire samples, the chemical bonding restricts the MoS₂ film from morphology change, and the coupling with the substrate has a relatively small influence on the A_{1g} mode. Therefore, we can conclude that the morphology of MoS₂ films plays a significant role in temperature dependence of A_{1g} mode, which leads to the large and highly non-linear deviation from the bulk, while the bonding between film and substrate introduces weaker effects, in similar magnitudes, to both E_{2g}^1 and A_{1g} modes on their temperature induced Raman shifts.

The integrated Raman intensity for both E_{2g}^1 and A_{1g} modes has been found to decrease in all CVD-grown samples when T is greater than 400 °C, possibly due to the decomposition of MoS₂ films. The thermal decomposition temperature for most samples including bulk is somewhere > 500 °C, except for 2L-CVD-SiO₂ being near 450 °C. For all CVD-grown MoS₂ films on sapphire, no Raman signal is detected when the temperature reaches 575 °C, indicating the decomposition of MoS₂ films. The Raman spectrum does not recover at room temperature after reaching the maximum temperature. The main change is that the frequency difference between A_{1g} and E_{2g}^1 modes increases by 2.5 cm⁻¹ for 1L-ME-SiO₂. In addition, their peak intensities decrease. There are at least two possible reasons: (1) the strain or morphology has changed, as expected, (2) the sample might be partially oxidized or decomposed. Similar results have been reported for graphene.³⁰

Simulation model for temperature dependence of Raman shift

The intrinsic temperature dependence of the Raman shift can be divided into thermal expansion of the lattice ($\Delta\omega_E$) and an anharmonic effect ($\Delta\omega_A$) which causes the change of phonon self-energy.^{27, 31, 32} In addition, thermally induced strains due to thermal expansion coefficient mismatch ($\Delta\omega_M$) between MoS₂ film and substrate should be considered.²⁸ Thus, the measured frequency change can be written as

$$\Delta\omega(T) = \Delta\omega_E(T) + \Delta\omega_A(T) + \Delta\omega_M(T), \quad (2)$$

where T is the sample temperature. Firstly, with increasing temperature, the lattice constant of MoS₂ structure increases due to thermal expansion of the film, leading to the Raman shift which is commonly expressed as³²

$$\Delta\omega_E(T) = \omega_0 \exp\left(-n\gamma \int_{25}^T \alpha \, dT\right) - \omega_0, \quad (3)$$

where ω_0 is the room temperature frequency, n is the degeneracy, 1 for A_{1g} mode and 2 for E_{2g}^1 mode, γ is the Gruneisen parameter, and α is the thermal expansion coefficient of the material. The Gruneisen parameters of both E_{2g}^1 and A_{1g} modes for bulk MoS₂ are $\gamma(E_{2g}^1) = 0.21$ and $\gamma(A_{1g}) = 0.42$, respectively. The in-plane and out-of-plane thermal expansion coefficients for bulk MoS₂ have been derived from the results of Ref.³³:

$$\alpha_a(T) = \left(\frac{0.6007 \times 10^{-5} + 0.6958 \times 10^{-7} T}{a} \right) \left(\frac{1}{^\circ\text{C}} \right) \\ \alpha_c(T) = \left(\frac{0.1064 \times 10^{-3} + 1.5474 \times 10^{-7} T}{c} \right) \left(\frac{1}{^\circ\text{C}} \right), \quad (4)$$

where T is the temperature in °C, a and c are the lattice constants of MoS₂ in Å. They are calculated to be 2.48×10^{-6} /°C and 9.14×10^{-6} /°C, respectively, for in-plane and out-of-plane thermal expansion coefficients at room temperature. The second term of right-handed side in Eq.(2) is related to pure temperature effect, so called “self-energy” shift due to anharmonic coupling of multiple phonons, which can be written as³¹

$$\Delta\omega_A(T) = A \left(1 + \frac{2}{e^x - 1} \right) + B \left(1 + \frac{3}{e^y - 1} + \frac{3}{(e^y - 1)^2} \right), \quad (5)$$

where $x = \hbar\omega/2kT$, $y = \hbar\omega/3kT$, and the first term corresponds to coupling of the optical phonon to two identical phonons, and the second term represents the coupling to three identical phonons. The coefficients A and B are constants that can be estimated by fitting the frequency shift attributes to anharmonic coupling. The possible remaining change of Raman shift is associated with the thermal expansion coefficient mismatch between film and substrate, introducing strain to the film, which can be expressed as²⁸

$$\Delta\omega_M(T) = \beta \int_{25}^T (\alpha_{sub}(T) - \alpha_{MoS_2}(T)) \, dT, \quad (6)$$

where β is the biaxial strain coefficient, α_{sub} and α_{MoS_2} are the thermal expansion coefficients of substrate and MoS₂, respectively. For bulk MoS₂, there is no thermal expansion

coefficient mismatch between MoS₂ layers, so that the third term is zero. Eq.(6) assumes that the film and substrate is in coherent strain, which is likely invalid for the transferred film. Fig.6 shows these contributions to the changes in Raman peak positions of both E_{2g}^I and A_{1g} modes for bulk MoS₂ with good agreement to experimental results. Table 2 shows the fitting parameters of A and B for both E_{2g}^I and A_{1g} modes.

However, this model, which predicts a monotonic behavior, is not appropriate for MoS₂ films, either 1L or 2L, on substrates. In the case of MoS₂ films on substrates like SiO₂/Si and sapphire, according to Eq.(6) with β being -2.1 cm^{-1} per % strain, the contribution of the thermal expansion coefficient mismatch is expected to be negligible compared to the thermal expansion of lattice and anharmonic effect in the temperature region of interest.^{34, 35} With increasing temperature, the biaxial tensile or compressive strain induced by thermal expansion coefficient mismatch increases significantly over the Van der

Table 2 The fitting parameters A and B for both E_{2g}^I and A_{1g} modes used in three- and four-phonon coupling model.

bulk MoS ₂	$A \text{ (cm}^{-1}\text{)}$	$B \text{ (cm}^{-1}\text{)}$
E_{2g}^I	-3.05835	0.04204
A_{1g}	-5.68777	0.26566

Waals force, resulting in the slippage or realignment of MoS₂ films on the surface of the substrate as well as forming wrinkles or ripples. For 1L-ME-SiO₂ sample, the realignment process takes place at $\sim 100^\circ\text{C}$ where there is an obvious slope transition of A_{1g} peak position. During the realignment process, defects may be introduced into MoS₂ film such as the breakdown of Mo-S bonds and the slow decomposition of the film, showing a broadening of A_{1g} Raman peak (Fig.4). After the MoS₂ layer adjusts to a stable state on the SiO₂/Si substrate at high temperature, the Raman shift of A_{1g} mode again follows what is expected from Eq.(2).

Full Width at Half Maximum (FWHM)

Fig.7 shows the temperature dependent FWHM of both E_{2g}^I peak and A_{1g} peak for all samples, by fitting to a Lorentzian lineshape function. Bulk MoS₂ has room-temperature FWHMs of 1.6 cm^{-1} and 2.2 cm^{-1} , respectively, for E_{2g}^I and A_{1g} . Other samples have greater FWHMs, indicating the film-substrate coupling and defects existing in these samples that cause the peak broadening. The FWHM of E_{2g}^I mode, in general, increases linearly with increasing temperature. However, the A_{1g} mode does not show a monotonic dependence but with a maximum linewidth in the middle of the temperature range. As it is discussed above, the mismatch of thermal expansion coefficients between MoS₂ films and substrates gives rise to changes of morphology e.g. wrinkles or ripples, consequently leading to a significant change of the temperature coefficients of A_{1g} mode. For all 1L and 2L samples, the FWHM of A_{1g} reaches the maximum when the realignment process occurs.

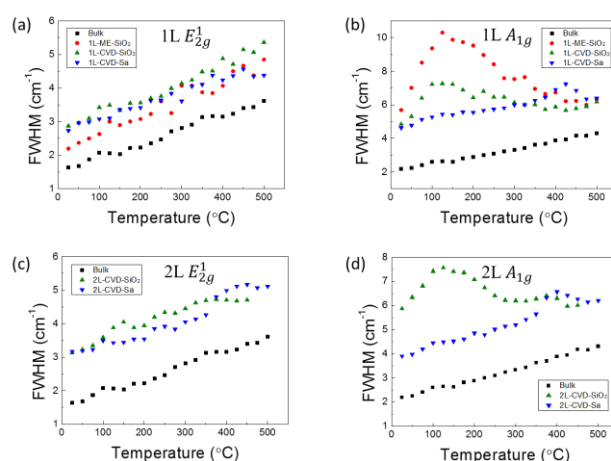


Fig. 7 Temperature dependence of FWHM of E_{2g}^I and A_{1g} modes in bulk and all other 1L and 2L samples.

For instance, the anomaly of temperature dependent Raman shift of 1L-ME-SiO₂ takes places at the temperatures starting from $\sim 100^\circ\text{C}$, while the FWHM reaches the maximum at 125°C and then starts to decrease afterward. This gives an additional illustration that the change of the morphology by the thermal expansion coefficient mismatch can affect the out-of-plane vibrational mode more than the in-plane mode when the temperature reaches a critical value.

Conclusions

In summary, we have reported temperature-dependent Raman studies of the in-plane E_{2g}^I and out-of-plane A_{1g} modes on single- and bi-layer MoS₂ samples prepared by CVD growth and mechanical exfoliation on SiO₂/Si and sapphire substrates in a temperature range of $25 - 500^\circ\text{C}$. Bulk MoS₂ has also been measured to serve as the references, with the first-order temperature coefficients of the Raman frequency shifts given as $\chi_1(E_{2g}^I) = -0.0221 \pm 8.9 \times 10^{-4} \text{ cm}^{-1}/\text{K}$ and $\chi_1(A_{1g}) = -0.0197 \pm 8.94 \times 10^{-4} \text{ cm}^{-1}/\text{K}$, respectively, for the E_{2g}^I and A_{1g} mode. The thermal decomposition temperature is found to be approximately 575°C for CVD-grown films on sapphire. The film-substrate coupling affects the temperature dependence of Raman frequency, intensity, and linewidth for both E_{2g}^I and A_{1g} modes in the 1L and 2L MoS₂. The impact depends on the substrate type and/or film-substrate binding mechanism. For the CVD grown film on the original sapphire substrate with likely chemical bonding between them, the film-substrate coupling significantly reduces the linear temperature coefficients of the Raman shift of the E_{2g}^I mode to $-0.0143 \pm 5.7 \times 10^{-4} \text{ cm}^{-1}/\text{K}$ for 1L and $-0.0135 \pm 8.4 \times 10^{-4} \text{ cm}^{-1}/\text{K}$ for 2L, but has no or small effect on the A_{1g} mode, with $-0.0199 \pm 0.0012 \text{ cm}^{-1}/\text{K}$ for 1L and $-0.0160 \pm 0.0014 \text{ cm}^{-1}/\text{K}$ for 2L. For the transferred film on SiO₂/Si substrate, originally grown on sapphire by CVD, for the E_{2g}^I mode, the temperature coefficients were found to be very close to the bulk value as $-0.0217 \pm 0.0017 \text{ cm}^{-1}/\text{K}$ for 1L and $-0.0233 \pm 0.0018 \text{ cm}^{-1}/\text{K}$ for 2L; but for A_{1g} mode, they increase substantially to $-0.0301 \pm 0.0023 \text{ cm}^{-1}/\text{K}$ for 1L and $-0.0310 \pm$

0.0018 cm⁻¹/K for 2L. The substrate effects are most pronounced for the A_{1g} mode, showing as stronger nonlinearity on the temperature shift of the Raman frequency and non-monotonic temperature dependence of the Raman linewidth. Similar or even stronger effects were observed on a mechanically exfoliated 1L film from a bulk single crystal. These results suggest that for the mechanically transferred thin film, due to the mismatch in thermal expansion between the film and substrate, the temperature change can lead to significant changes in the thin-film morphology as a result of realignment of the film on the substrate, which can be most easily probed by the temperature dependence of the A_{1g} mode associated with the out-of-plane atomic vibration. Temperature dependent Raman study provides an efficient tool for investigating the coupling between the 2-D material and substrate either with chemical or mechanical bonding.

Acknowledgements

Y.Z. acknowledges the support of Bissell Distinguished Professorship. L.C. acknowledges the support of a Young Investigator Award from the Army Research Office (W911NF-13-1-0201).

Notes and references

^a Electrical and Computer Engineering Department, University of North Carolina at Charlotte, Charlotte, NC 28223, USA. Email: yong.zhang@uncc.edu

^b Department of Materials Science and Engineering, North Carolina State University, Raleigh, NC 27695, USA.

† Electronic Supplementary Information (ESI) available: The temperature-dependent Raman of another two mechanically exfoliated 1L MoS₂ films on SiO₂/Si substrate. See DOI: 10.1039/b000000x/

1. K. S. Novoselov, A. K. Geim, S. V. Morozov, D. Jiang, M. I. Katsnelson, I. V. Grigorieva, S. V. Dubonos and A. A. Firsov, *Nature*, 2005, 438, 197-200.
2. Y.-M. Lin, C. Dimitrakopoulos, K. A. Jenkins, D. B. Farmer, H.-Y. Chiu, A. Grill and P. Avouris, *Science*, 2010, 327, 662.
3. F. Schwierz, *Nat Nano*, 2010, 5, 487-496.
4. K. S. Novoselov, A. K. Geim, S. V. Morozov, D. Jiang, Y. Zhang, S. V. Dubonos, I. V. Grigorieva and A. A. Firsov, *Science*, 2004, 306, 666-669.
5. K. Watanabe, T. Taniguchi and H. Kanda, *Nat Mater*, 2004, 3, 404-409.
6. C. Jin, F. Lin, K. Suenaga and S. Iijima, *Physical Review Letters*, 2009, 102, 195505.
7. I. Meric, M. Y. Han, A. F. Young, B. Ozyilmaz, P. Kim and K. L. Shepard, *Nat Nano*, 2008, 3, 654-659.
8. Y.-W. Son, M. L. Cohen and S. G. Louie, *Physical Review Letters*, 2006, 97, 216803.
9. G. Giovannetti, P. A. Khomyakov, G. Brocks, P. J. Kelly and J. van den Brink, *Physical Review B*, 2007, 76, 073103.
10. Y. Zhang, T.-T. Tang, C. Girit, Z. Hao, M. C. Martin, A. Zettl, M. F. Crommie, Y. R. Shen and F. Wang, *Nature*, 2009, 459, 820-823.
11. Y. Kubota, K. Watanabe, O. Tsuda and T. Taniguchi, *Science*, 2007, 317, 932-934.
12. K. F. Mak, C. Lee, J. Hone, J. Shan and T. F. Heinz, *Physical Review Letters*, 2010, 105, 136805.
13. A. Splendiani, L. Sun, Y. Zhang, T. Li, J. Kim, C.-Y. Chim, G. Galli and F. Wang, *Nano Letters*, 2010, 10, 1271-1275.
14. RadisavljevicB, RadenovicA, BrivioJ, GiacomettiV and KisA, *Nat Nano*, 2011, 6, 147-150.
15. Y. Zhan, Z. Liu, S. Najmaei, P. M. Ajayan and J. Lou, *Small*, 2012, 8, 966-971.
16. Y. Yu, C. Li, Y. Liu, L. Su, Y. Zhang and L. Cao, *Sci. Rep.*, 2013, 3.
17. A. Molina-Sánchez and L. Wirtz, *Physical Review B*, 2011, 84, 155413.
18. E. S. Kadantsev and P. Hawrylak, *Solid State Communications*, 2012, 152, 909-913.
19. X. Zhang, W. P. Han, J. B. Wu, S. Milana, Y. Lu, Q. Q. Li, A. C. Ferrari and P. H. Tan, *Physical Review B*, 2013, 87, 115413.
20. M. Ghorbani-Asl, N. Zibouche, M. Wahiduzzaman, A. F. Oliveira, A. Kuc and T. Heine, *Sci. Rep.*, 2013, 3.
21. H. Li, Q. Zhang, C. C. R. Yap, B. K. Tay, T. H. T. Edwin, A. Olivier and D. Baillargeat, *Advanced Functional Materials*, 2012, 22, 1385-1390.
22. A. C. Ferrari, J. C. Meyer, V. Scardaci, C. Casiraghi, M. Lazzeri, F. Mauri, S. Piscanec, D. Jiang, K. S. Novoselov, S. Roth and A. K. Geim, *Physical Review Letters*, 2006, 97, 187401.
23. S. Sahoo, A. P. S. Gaur, M. Ahmadi, M. J. F. Guinel and R. S. Katiyar, *The Journal of Physical Chemistry C*, 2013, 117, 9042-9047.
24. S. Najmaei, P. M. Ajayan and J. Lou, *Nanoscale*, 2013, DOI: 10.1039/C3NR02567E.
25. P. G. Klemens, *Physical Review*, 1966, 148, 845-848.
26. L. A. Falkovsky, *J. Exp. Theor. Phys.*, 2007, 105, 397-403.
27. I. Calizo, A. A. Balandin, W. Bao, F. Miao and C. N. Lau, *Nano Letters*, 2007, 7, 2645-2649.
28. D. Yoon, Y.-W. Son and H. Cheong, *Nano Letters*, 2011, 11, 3227-3231.
29. Y. y. Wang, Z. h. Ni, T. Yu, Z. X. Shen, H. m. Wang, Y. h. Wu, W. Chen and A. T. Shen Wee, *The Journal of Physical Chemistry C*, 2008, 112, 10637-10640.
30. Z. H. Ni, H. M. Wang, Z. Q. Luo, Y. Y. Wang, T. Yu, Y. H. Wu and Z. X. Shen, *Journal of Raman Spectroscopy*, 2010, 41, 479-483.
31. M. Balkanski, R. F. Wallis and E. Haro, *Physical Review B*, 1983, 28, 1928-1934.
32. J. Menéndez and M. Cardona, *Physical Review B*, 1984, 29, 2051-2059.
33. S. H. El-Mahalawy and B. L. Evans, *Journal of Applied Crystallography*, 1976, 9, 403-406.
34. H. Tada, A. E. Kumpel, R. E. Lathrop, J. B. Slanina, P. Nieva, P. Zavracky, I. N. Miaoulis and P. Y. Wong, *J Appl Phys*, 2000, 87, 4189-4193.
35. C. Rice, R. J. Young, R. Zan, U. Bangert, D. Wolverson, T. Georgiou, R. Jalil and K. S. Novoselov, *Physical Review B*, 2013, 87, 081307.